Electron-Withdrawing Ability Tunable Polyphosphazene Frameworks as Novel "Heterogreeneous" Catalysts for Efficient Biomass Upgrading†

Zhen Huang,‡[a] Yuan-Jia Pan,‡[b] Jia Guo,[b] Wei Shen,[a] Yimin Chao,[c] Chang-Chun Wang*[b] and Hua-Long Xu*[a]

The structure variety and functionalization flexibility of polymers extend the portfolio of catalysts for biomass transformation to chemicals and biofuels. In this work, we have successfully produced a series of polyphosphazene nano- frameworks based on hexachlorocyclotriphosphazene which exhibited high activity as non-acidic heterogeneous catalysts for dehydration of fructose to 5-hydroxymethylfurfural under mild conditions. These polymeric frameworks possess tunable electron-withdrawing capability with high chemical and thermal stability as well as good recyclability by introducing co-monomers with different structures. It is revealed that the unique cyclotriphosphazene unit and electron-withdrawing nature of polymer backbone are essential for the catalytic performance. This strategy has provided a new pathway to designing highly active and environmentally friendly heterogeneous catalysts and innovative technologies for biomass conversion.

Platform molecules from renewable biomass resources are a promising alternative to those from petrochemical refining processes, which can be upgraded to a broad range of energy and chemical materials.1-7 In particular, 5-hydroxymethylfurfural (HMF), as one of the top building-blocks, can be converted to not only high valued 2,5-disubstituted furan derivatives used for production of fuels, fine chemicals and polymers, but also other platform molecules such as levulinic acid (LA) and 2,5-diformylfuran (DFF).8-10 It has been identified that the production of HMF can undergo a catalytic dehydration of carbohydrates based on C6 units in acidic mediums,11-13 however the HMF yield is limited by the formation of soluble polymers and insoluble humins, and by water induced HMF rehydration. Although it is afterwards improved by introducing organic solvents (i.e. dimethyl sulfoxide) to the process,14-16 the corrosivity, together with the complex and high energy consumption isolation procedures, is the most significant barrier to their industrial applications.

Later, the applications of ionic liquids (ILs) have drawn much attention in the production of bio-derived platform molecules, because efficient conversion with high selectivity can be achieved where ILs act as the catalysts and/or the solvents to avoid the use of acids.17 For instance, sugars can be selectively dehydrated into HMF by the metal chlorides, such as $CrCl_3$ and VCl_3, in ILs with or without using acids.18-20 But the use of these metals caused extremely serious environmental issues. Although much work have been devoted to replacing them with less or none toxic catalysts,21-24 the high cost and the low recyclability of the catalysts in the ILs involved processes are unavoidable challenges in their applications.

From the view of environmentally friendly and cost-effective biomass utilization, heterogeneous catalysts should be more desired due to their flexible acidity, inexpensive production and facile recovery. Accordingly, H-form zeolites,25,26 as well as other solid acidic catalysts including acidic ion-exchange resin,27-31 acid- functionalized silica, TiO_2 and ZrO_2,32-34 supported heteropolyacid35 and solid metal phosphate,36 have been extensively investigated and shown some competitive activities and reusability in conversion of sugars into HMF and other chemicals. On the other hand, the recently developed continuous reaction processes have greatly improved the application of heterogeneous catalysts.7,37 However, the efficiency is relatively low even under a high temperature. Therefore, to realize a feasible chemical engineering process for biomass conversion, a high activity and environmentally friendly catalyst system with low cost and convenient applicability is under tremendous demand at present.

More recently, functionalized polymer materials have been successfully applied in platform molecules production from biomass, whose catalytic performance are not only effected by the active sites but the character of the structure as well.30,38 In our previous work, triazaheterocyclic compounds, like hexachlorocyclotriphosphazene (HCCP) and cyanuric chloride (CNC), are found as efficient homogeneous catalysts for dehydration of fructose to HMF under mild conditions, whose activity might be effected by the electronic effect of the substituents.39 Herein, based on the nature of HCCP in synthesizing stable and degradable polymers,40,41 we have successfully designed and synthesized a series of novel polyphosphazene nanoparticles (PZS-NPs), with different co- monomers including 4,4'-sulfonyldiphenol (BPS), 4,4'-(hexafluoro- isopropylidene) diphenol (BPAF) and 4,4'-diamino-diphenyl ether (ODA), as heterogeneous catalysts for the dehydration reaction, which are reliable for recycling and allow the conversion of sugar under mild conditions. To be emphasized, PZS-NPs can activate fructose for its highly efficient dehydration, and exhibit a performance superior to HCCP, which can be contributed to the improvement by the electron-withdrawing nature of the polymeric framework.

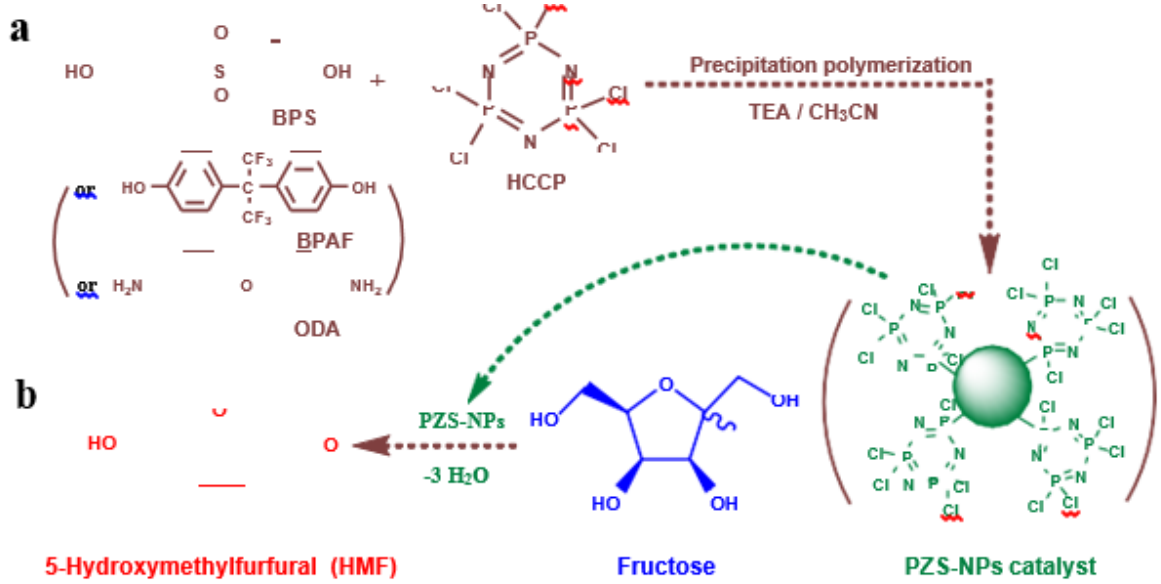

Scheme 1. Schematic illustration of (a) proposed preparation of PZS-NPs and (b) their applications in the catalyzed conversion of fructose to HMF.

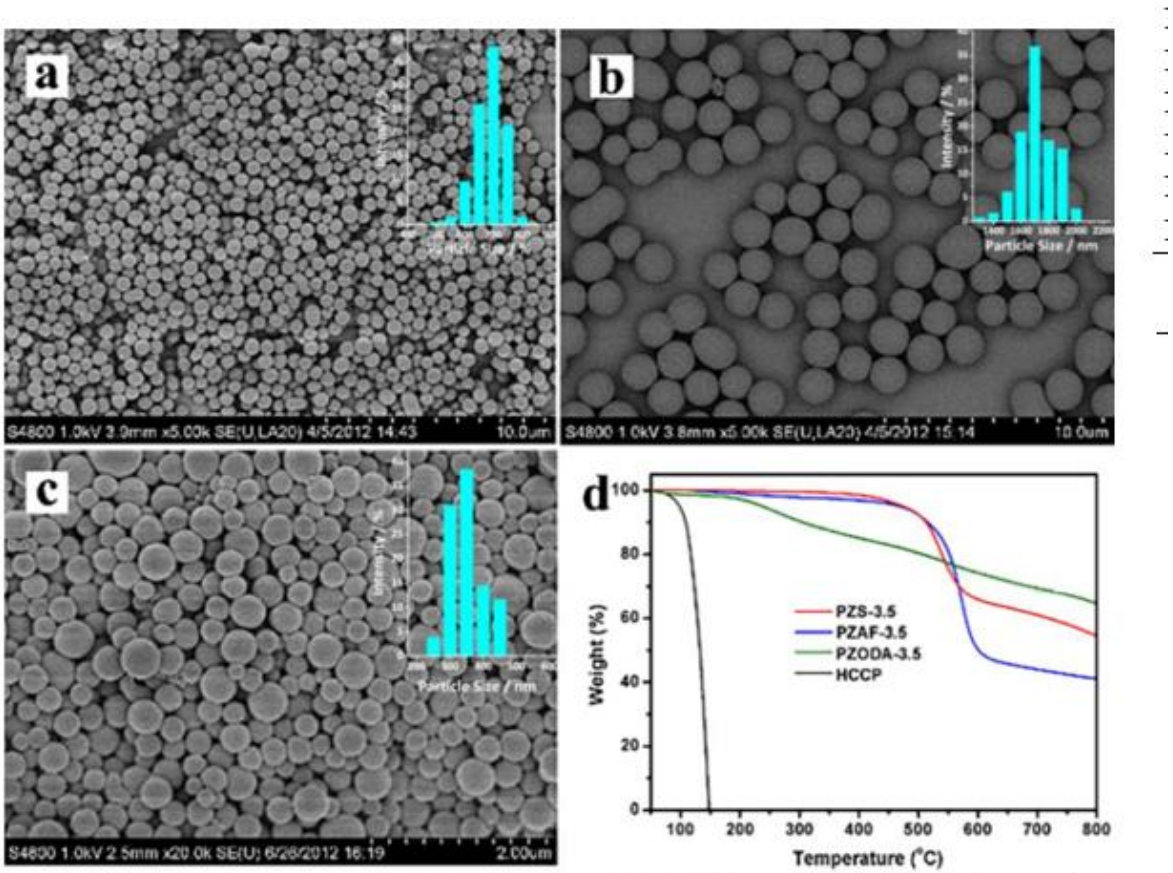

Fig. 1 FE-SEM images of (a) PZS-3.5; (b) PZAF-3.5; (c) PZODA-3.5 and (d) TGA curves of PZS-3.5, PZAF-3.5, PZODA-3.5 and HCCP, respectively. Insets a – c: primary particle size distributions estimated from more than 200 particles for each sample.

In this work, poly(cyclotriphosphazene-co-4,4'-sulfonyldiphenol) nanoparticles, was synthesized by a precipitation polymerization of BPS and HCCP (BPS : HCCP = 3.5 : 1) in the presence of triethyl-amine (TEA) in acetonitrile at room temperature (Scheme 1). By taking the electronic effect of substituents into account, two different co-monomers, BPZF and ODA, were adopted instead of BPS, and thus poly(cyclotriphosphazene-co-(4,4'-(hexafluoroisopropylidene) diphenol)) nanoparticles and poly(cyclotriphosphazene-co-(4,4'- diaminodiphenyl ether)) nanoparticles were successfully produced with the same route. We denoted these three frameworks as PZS-3.5, PZAF-3.5 and PZODA-3.5, respectively. From Field Emission Scanning Electron Microscope (FE-SEM) images (Fig. 1a-c), three polymeric frameworks showed a uniform spherical morphology, and have a narrow size distribution of approximately 700 nm, 1700 nm and 350 nm for PZS, PZAF and PZODA, respectively. Energy dispersive X-ray spectroscopy (EDX) and FTIR spectra revealed the abundant P, Cl, S (or F, N) elements and the characteristic absorption bands of polyphosphazene, confirming the compositions derived from the used monomers (Fig. S1 and S2). In addition, thermo-gravimetric analysis (TGA) verified the thermal stability of PZS-NPs with a high decomposition temperature in nitrogen over 400 oC, in a sharp contrast to the monomer of HCCP and co- monomers (Fig. 1d & Fig. S3). Also, by tuning the feeding ratios of BPS and HCCP, we successfully synthesized a series of PZS nanoparticles with different compositions, which denoted as PZS-X (X indicates the molar ratio of BPS to HCCP). As one can observe, all the samples showed a well-dispersed particle size, which however gradually increased as the increasing concentration of BPS (Fig. S4).

Table 1. Dehydration of fructose to HMF by PZS-NPs and other relative catalysts under different conditions.[a]

Entry	Catalyst	Catalyst dosage (g)	Fructose Content (g / wt%)	HMF Yield (%)
1	PZS-3.5	0.2	0.375/3	95.4
2	PZS-2.0	0.2	0.375/3	97.2
3	PZS-5.5	0.2	0.375/3	90.2
4	PZS-7.0	0.2	0.375/3	81.9
5	HCCP[b]	0.0395	0.375/3	90.7
6	HCl	0.0249	0.375/3	91.4
7	BPS	0.2	0.375/3	Trace
8	PZAF-3.5	0.2	0.375/3	96.4
9	PZODA-3.5	0.2	0.375/3	82.2
10	None	--	0.375/3	trace
11	PZS-2.0	2.0	3.75/30	85.9
12	PZS-3.5	2.0	3.75/30	78.7
13	PZS-5.5	2.0	3.75/30	60.1
14	PZS-7.0	2.0	3.75/30	55.9
15	None	--	3.75/30	trace

[a] Reaction conditions: 90 °C, 0.5 h, in DMSO; [b] The dosage was adopted based on the Cl content of PZS-2.0.

Dehydration reactions were firstly carried out over PZS-3.5 in a 3 wt% fructose-DMSO solution at 90 oC for 0.5 h. Evidently, PZS-3.5 exhibited outstanding catalytic performance in conversion of fructose to HMF, with a 95.4 % yield of HMF (Table 1, entry 1). Moreover, this catalyst could possess high efficiency under lower temperature, and a 92.3 % of HMF yield was achieved by PZS-3.5 even at 50 oC after 10 h (Fig. S5). Moreover, when the feeding molar ratios were varied from 2:1 to 7:1, the catalytic activity of PZS-NPs was reduced correspondingly (entry 1-4). And an even better HMF yield of 97.2 % was obtained for PZS-2.0 under the same reaction conditions, in which HCCP took over the highest content in all the PZS frameworks. It is naturally speculated that the dangling P-Cl groups on the periphery of PZS-NPs are varied in number with addition of nonstoichiometric BPS in synthesis, and the un- terminated HCCP moiety should take effect in catalytic reaction, which was in accordance with our previous work39. Furthermore, it is worth noting that the superiority of PZS-NPs was revealed by showing a better performance than HCCP and HCl (Table 1, entry 5 & 6, Fig. S6) after we compared the catalytic activity of the polymers with that of HCCP based on the same chlorine content of PZS-2.0 (Table S1), while a sharp decrease of the yield of HMF was appeared when using BPS as catalyst (entry 7). To further elucidate their variation, we utilized the catalysts of PZS-2.0, HCCP and HCl to undergo the dehydration reaction at a lower reaction temperature of 60 oC (Fig. S6). It is evident that though parts of active catalytic sites have been buried inside the PZS-NPs, the catalytic performance of PZS-2.0 is more distinct than those of the homogeneous catalysts HCCP and HCl under different reaction times and temperatures. In conclusion, this result implied that HCCP not only endow PZS-NPs with the prominent catalytic activity, but its activity meanwhile might be enhanced by the structure of polymer after the polymerization.

Apart from the exceptional catalytic ability of P-Cl groups in PZS- NPs, synergistic role of polymer backbones within PZS-NPs might exist in catalysis procedure, in particular when taking into account the difference in catalytic performance of HCCP and PZS-NPs.42 Accordingly, based on HCCP monomer, PZAF-3.5 and PZODA-3.5, two kinds of derivatives of PZS-NPs with different electronic properties were synthesized to investigate the cooperative impact of polymers. As a result, PZAF-3.5 showed a superior catalytic performance on dehydration of fructose with a HMF yield of 96.4 % after a reaction time of 0.5 h compared with that of PZS-3.5, while PZODA-3.5 possessed a inhibited activity under the same conditions (Table 1, entry 8 & 9). Astoundingly, PZAF-3.5 had enabled the dehydration with a very high rate, leading to a HMF yield of 83.1 % after a short reaction time of only 5 min, which was much better than that of PZS-3.5 under the same conditions (Fig. 2). In contrast, the HMF yield for PZODA-3.5 was only 9.9% after 5 min and only reached 82.2% after 0.5 h, whose catalytic activity was slightly inferior to that of HCCP. This difference could be ascribed to the enhancement from -CF3 groups of 4,4'-(hexafluoroisopropylidene) diphenol in the framework of PZAF-3.5 conferring a stronger electron-withdrawing capability as compared with the sulfone groups of 4,4'-sulfonyldiphenol in PZS-3.5, which resulted in an more electron-positive phosphor centre and stronger interactions (i.e. hydrogen bonds) between PZAF and fructose/intermediates. On the other hand, the ether unit 4,4'-diaminodiphenyl ether as well as the tertiary amine groups in the framework of PZODA-3.5 showed a weak electron-donating capacity, which is negative in activating the P-Cl sites against the efficient generation of HMF. Thus the catalytic sites stemming from P-Cl groups are accordingly activated by virtue of the electro-migration capability of polymer backbone, which makes PZAF and PZS nanoparticles a potential alternative to homogeneous acid catalysts for the industrial applications.

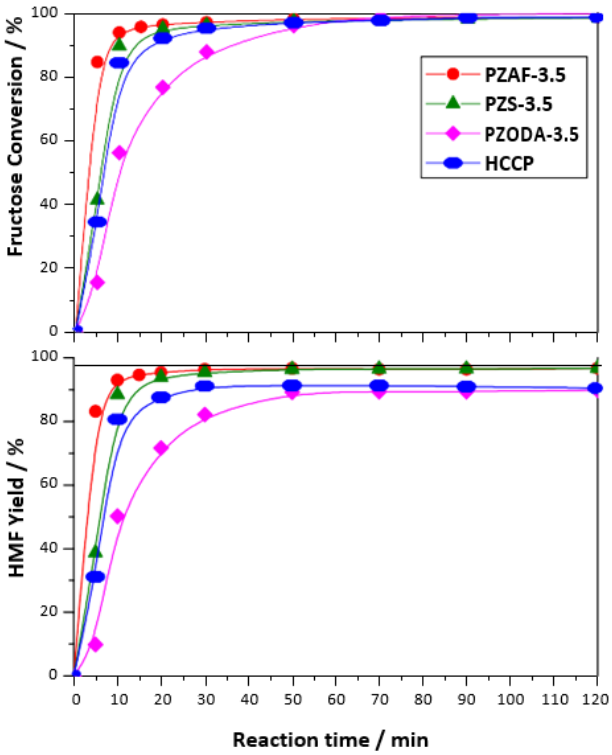

Fig. 2 The catalytic performances of PZAF-3.5, PZS-3.5, PZODA-3.5 and HCCP on dehydration of fructose to HMF. (Conditions: 12.5 g 3 wt% fructose/DMSO, 90 °C, 2 h; 0.2 g catalyst for PZS-NPs and 10.6 mg catalyst for HCCP.)

As we know, the concentration of fructose in reaction system is of paramount significance in the practical application. Herein, dehydration of fructose at high concentration was conducted (Table 1, entry 11-15). When dehydration of 30 wt% fructose was catalysed by PZS-2.0, the HMF yield reached 85.9%, unequivocally higher than the reported best yield (approximately 76%)3,5. With decreases in feeding ratios of HCCP and BPS, the catalytic activity of resulting PZS-NPs was reduced as well, which same as the tendency was found at a low fructose concentration.

With these all in mind, a possible catalytic mechanism of PZS-NPs catalysed dehydration of fructose illustrated in Scheme 2 was proposed based on our previously reported results.39 The O-triazine intermediate (A) was firstly formed on the surface of PZS-NPs, followed by the protonation step to form intermediate B and then the formation of 2-hydroxymethyl-5-hydroxylmethylene-tetrahydro-furan-3,4-diol. HMF was finally generated after the loss of the two water molecules. During the process, the interactions between PZS- ZPs and fructose as well as intermediate products should provide an enhancement in each dehydration step.

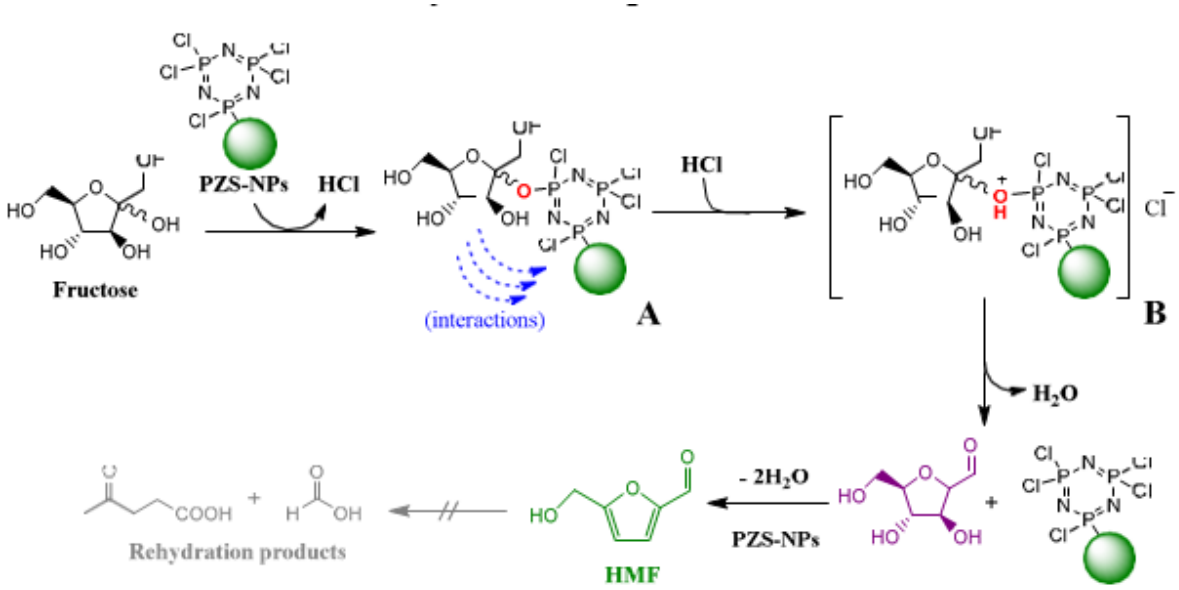

Scheme 2. Proposed reaction mechanism for dehydration of fructose to HMF catalyzed by polyphosphazene nanoparticles.

Finally, reusability and recyclability of PZS-NPs were evaluated as well on PZS-2.0, and the experimental results were compiled in Table 2. As expected, the selectivity of HMF was well kept after 5 cycles, and the catalytic activity of PZS-2.0 was decreased merely from 93.6% to 86.2%. However, the reduced active P-Cl groups due to site covering or substituted Cl should be responsible for the lost activity.

Table 2. Recycle of PZS-2.0 for catalytic conversion of fructose to HMF.[a]

Run	Conversion / %	Selectivity / %	HMF Yield / %
1	99.7	93.9	93.6
2	95.3	97.0	92.4
3	93.4	97.0	90.6
4	92.0	96.8	89.1
5	90.6	95.1	86.2

[a] 10 wt% fructose in DMSO, 90 °C, 0.5 h

In summary, a heterogeneous catalyst of polyphosphazene nanoparticles has been developed for highly efficient conversion of fructose to HMF. Under relatively mild conditions, HMF was produced with 97.2% yield in 3 wt% fructose solution and 85.9% yield in 30 wt% fructose solution at 90 oC for 0.5 h, which is the first example concerning polymeric nanoparticle catalysts used for fructose conversion. Moreover, it has been substantially verified that the as-prepared polyphosphazene nanoparticle catalyst possesses the following outstanding properties: (1) unique electron-withdrawing polymer backbone activating the P-Cl catalytic sites for a much higher catalytic activity; (2) high selectivity, recyclability and stability; (3) being environmentally friendly without the utilizing strong proton acid and any metal. Therefore, the concept of structure-enhanced catalytic performance opens a new pathway for developing highly active, green and degradable heterogeneous catalysts, and efficient chemical technologies for dehydration of fructose to HMF and other biomass conversion as well.

Acknowledgements

We are grateful to Sino-UK higher education research partnership sponsored by British council and Chinese scholarship council. This work was supported by National Science Foundation of China (Grant No. 21474017), National Science and Technology Key Project of China (Grant No. 2012AA020204), Shanghai Science and Technology Committee (Grant No. 14DZ2273900) and the China Postdoctoral Science Foundation (Grant No. 2015M571487).

Notes and references

a Department of Chemistry, Shanghai Key Laboratory of Molecular Catalysis and Innovative Materials, Laboratory of Advanced Materials and Collaborative Innovation Center of Chemistry for Energy Materials, Fudan University, Shanghai 200433, P.R. China. E-mail: shuhl@fudan.edu.cn; Fax: +86-21-65641740

b Department of Macromolecular Science, State Key Laboratory of

Molecular Engineering of Polymers and Laboratory of Advanced Materials, Fudan University, Shanghai 200433, P.R. China. E-mail: ccwang@fudan.edu.cn; Fax: +86-21-65640293

c Energy Materials Lab, School of Chemistry, University of East Anglia,

Norwich, NR4 7TJ, UK

† Electronic Supplementary Information (ESI) available: Experimental details and supporting tables and figures. See DOI: 10.1039/c000000x/

‡ Contributed equally to this work.

1. J. N. Chheda, G. W. Huber and J. A. Dumesic, Angew. Chem. Int. Ed., 2007, 46, 7164-7183.

2. T. Wang, M. W. Nolte and B. H. Shanks, Green Chem., 2014, 16, 548- 572.

3. Y. Román-Leshkov, J. N. Chheda and J. A. Dumesic, Science, 2006, 312, 1933-1937.

4. I. Delidovich, K. Leonhard and R. Palkovits, Energy Environ. Sci., 2014, 7, 2803-2830.

5. Y. Román-Leshkov, C. J. Barrett, Z. Y. Liu and J. A. Dumesic, Nature, 2007, 447, 982-985.

6. S. G. Wettstein, D. M. Alonso, Y. Chong and J. A. Dumesic, Energy Environ. Sci., 2012, 5, 8199-8203.

7. R. Alamillo, A. J. Crisci, J. M. R. Gallo, S. L. Scott and J. A. Dumesic, Angew. Chem. Int. Ed., 2013, 52, 10349-10351.

8. D. Esposito and M. Antonietti, Chem. Soc. Rev., 2015, 44, 5821-5835.

9. A. A. Rosatella, S. P. Simeonov, R. F. M. Frade and C. A. M. Afonso, Green Chem., 2011, 13, 754-793.

10. A. Mukherjee, M.-J. Dumont and V. Raghavan, Biomass and Bioenergy, 2015, 72, 143-183.

11. H. E. van Dam, A. P. G. Kieboom and H. van Bekkum, Starch, 1986, 38, 95-101.

12. A. S. Amarasekara, L. D. Williams and C. C. Ebede, Carbohyd. Res., 2008, 343, 3021-3024.

13. G. R. Akien, L. Qi and I. T. Horvath, Chem. Commun., 2012, 48, 5850- 5852.

14. B. F. M. Kuster and J. Laurens, Starch, 1977, 29, 172-176.

15. M. J. Antal Jr, W. S. L. Mok and G. N. Richards, Carbohyd. Res., 1990,199, 91-109.

16. Y. Nakamura and S. Morikawa, B. Chem. Soc. Jpn., 1980, 53, 3705- 3706.

17. M. E. Zakrzewska, E. Bogel-Łukasik and R. Bogel-Łukasik, Chem. Rev., 2011, 111, 397-417.

18. H. Zhao, J. E. Holladay, H. Brown and Z. C. Zhang, Science, 2007, 316, 1597-1600.

19. G. Yong, Y. Zhang and J. Y. Ying, Angew. Chem. Int. Ed., 2008, 47, 9345-9348.

20. J. B. Binder and R. T. Raines, J. Am. Chem. Soc., 2009, 131, 1979-1985.

21. S. Hu, Z. Zhang, J. Song, Y. Zhou and B. Han, Green Chem., 2009, 11, 1746-1749.

22. F. Tao , H. Song and L. Chou, ChemSusChem, 2010, 3, 1298-1303.

23. E. A. Khokhlova, V. V. Kachala and V. P. Ananikov, ChemSusChem, 2012, 5, 783-789.

24. Z. Zhang, Q. Wang, H. Xie, W. Liu and Z. Zhao, ChemSusChem, 2011, 4, 131-138.

25. R. O'Neill, M. N. Ahmad, L. Vanoye and F. Aiouache, Ind. Eng. Chem. Res., 2009, 48, 4300 4306.

26. X. Qi, M. Watanabe, T. M. Aida and J. R. L. Smith, Green Chem., 2008, 10, 799-805.

27. Y. Peng, Z. Hu, Y. Gao, D. Yuan, Z. Kang, Y. Qian, N. Yan and D. Zhao, ChemSusChem, 2015, 8, 3208-3212.

28. S. Mondal, J. Mondal and A. Bhaumik, ChemCatChem, 2015, 7, 3570- 3578.

29. A. Takagaki, M. Ohara, S. Nishimura and K. Ebitani, Chem. Commun., 2009, 6276-6278.

30. Z. Huang, W.-Y. Pan, H.-B. Zhou, F. Qin, H.-L. Xu and W. Shen, ChemSusChem, 2013, 6, 1063-1069.

31. C. Moreau, R. Durand, S. Razigade, J. Duhamet, P. Faugeras, P. Rivalier, P. Ros and G. Avignon, Appl. Cata. A, 1996, 145, 211-224.

32. E. Kılıç and S. Yılmaz, Ind. Eng. Chem. Res., 2015, 54, 5220-5225.

33. A. J. Crisci, M. H. Tucker, M.-Y. Lee, S. G. Jang, J. A. Dumesic and S. L. Scott, ACS Catal., 2011, 1, 719-728.

34. P. Carniti, A. Gervasini, S. Biella and A. Auroux, Catal. Today, 2006, 118, 373-378.

35. Y. Liu, L. Zhu, J. Tang, M. Liu, R. Cheng and C. Hu, ChemSusChem, 2014, 7, 3541-3547.

36. M. A. Schwegler, P. Vinke, M. van der Eijk and H. van Bekkum, Appl. Cata. A, 1992, 80, 41-57.

37. M. H. Tucker, A. J. Crisci, B. N. Wigington, N. Phadke, R. Alamillo, J. Zhang, S. L. Scott and J. A. Dumesic, ACS Catal., 2012, 2, 1865-1876.

38. C. Tian, C. Bao, A. Binder, Z. Zhu, B. Hu, Y. Guo, B. Zhao and S. Dai, Chem. Commun., 2013, 49, 8668-8670.

39. Z. Huang, Y.-J. Pan, Y.-M. Chao, W. Shen, C.-C. Wang and H.-L. Xu, RSC Adv., 2014, 4, 13434-13437.

40. X. Wang, J. Fu, Z. Chen, Q. Li, X. Wu and Q. Xu, RSC Adv., 2015, 5, 33720-33728.

41. S. Wilfert, A. Iturmendi, W. Schoefberger, K. Kryeziu, P. Heffeter, W. Berger, O. Brüggemann and I. Teasdale, J. Polym. Sci. Pol. Chem., 2014, 52, 287-294.

42. P. Mohanty, L. D. Kull and K. Landskron, Nat. Commun., 2011, 2, 401.

Supporting information

Electron-Withdrawing Ability Tunable Polyphosphazene Frameworks as Novel "Heterogreeneous" Catalysts for Efficient Biomass Upgrading

Zhen Huang1, Yuan-Jia Pan2, Jia Guo2, Wei Shen1, Yimin Chao3, Chang-Chun Wang2* and Hua-Long Xu1*,

1) Department of Chemistry, Shanghai Key Laboratory of Molecular Catalysis and Innovative Materials, Laboratory of Advanced Materials and Collaborative Innovation Center of Chemistry for Energy Materials, Fudan University, Shanghai 200433, China

2) State Key Laboratory of Molecular Engineering of Polymers and Department of Macromolecular Science, Laboratory of Advanced Materials, Fudan University, Shanghai 200433, China

3) Energy Materials Lab, School of Chemistry, University of East Anglia, Norwich, NR4 7TJ, United Kingdom

Email: shuhl@fudan.edu.cn; ccwang@fudan.edu.cn

Materials:

Fructose was purchased from Sigma-Aldrich. Hexachlorocyclotriphosphazene (HCCP), 4,4'-sulfonyldiphenol (BPS), 4,4'- (hexafluoroisopropylidene) diphenol (BPAF), 4,4'-diaminodiphenyl ether (ODA), benzoyl chloride, and dihydroxyacetone were purchased from Aladdin Chemistry Co. Ltd (China). Acetonitrile (AN) (GC > 99.9%) was purchased from Shanghai Lingfeng Chemical Reagent Company and was used without further purification. Acetone, tetrahydrofuran (THF), triethylamine (TEA) and DMSO (analytical grade) were obtained from Shanghai Chemical Reagents Company and used without further purification. Dimethyl sulfoxide-D6 for NMR measurements was obtained from Cambridge Isotope Laboratories, Inc.

Preparation of poly(cyclotri-phosphazene-co-4,4'-sulfonyldiphenol) nanoparticles (PZS-NPs):

The typical preparation was carried out as follows: TEA (0.52 g, 5.14 mmol), HCCP (0.2 g, 0.575 mmol), and BPS with different feed ratios were added in a glass flask and dissolved in acetonitrile (50 ml) under ultrasonic irradiation, then the reaction was completed after 2 h at room temperature. The precipitated polymer nanoparticles were separated by filtration, and then washed with acetone,

ethanol and deionized water, respectively. The final products were dried in vacuum at 40 oC to a constant weight.

Preparation of poly(cyclotriphosphazene-co-(4,4'-(hexafluoroisopropylidene) diphenol)) nanoparticles (PZAF-NPs):

The preparation of PZAF-3.5 was carried out as follows (as shown in Scheme S1): TEA (0.52 g, 5.14 mmol), HCCP (0.1 g, 0.288 mmol), and BPAF (0.34 g, 1.008 mmol) were added in a glass flask and dispersed in acetonitrile (50 ml) under ultrasonic irradiation. The reaction was completed after 3 h at room temperature. The precipitated polymer nanoparticles were recovered by filtration, washed with acetone, ethanol and deionized water, and then dried in vacuum at 40 oC to a constant weight.

Preparation of poly(cyclotriphosphazene-co-(4,4'-diaminodiphenyl ether)) nanoparticles (PZODA-NPs):

The preparation of PZODA-3.5 was carried out as follows (as shown in Scheme S2): TEA (0.52 g, 5.14 mmol), HCCP (0.1 g, 0.288 mmol), and ODA (0.202 g, 1.008 mmol) were added to a glass flask and dispersed in acetonitrile (50 ml) under ultrasonic irradiation. The reaction was completed after 8 h at 60 oC. The precipitated polymer nanoparticles were recovered by filtration, washed with acetone, ethanol and deionized water, and then dried in vacuum at 40 oC to a constant weight.

Catalyst recycling experiments:

12.5 g of 10 wt% fructose/DMSO was mixed with 0.67 g PZS-2.0 in a 50 ml flash equipped with magnetic stirring, and the reaction was kept in oil bath at 90 oC for 0.5 h. After that, the nanoparticle catalyst was separated by centrifugation and purified for three times by repeating ultra-centrifugation (12,000 rpm for 10 min) / re-dispersion cycles in acetonitrile with ultrasonic bathing and was dried in a vacuum at 45oC overnight. It was then used directly for the next run by adding the sugar.

Typical separation procedure for HMF：

After the dehydration reaction of fructose, the reaction mixture was centrifugation and then filtration to separate the polymer catalyst, then the liquid was transferred into a flask and was distilled under reduced pressure to remove the DMSO solvent. The remaining mixture was extracted with ethyl acetate (20 mL×5) after water (20 mL) was added, and then the organic phase was collected. After drying with anhydrous sodium sulfate, the organic layer was distilled under reduced pressure to obtain pure HMF as the main product. The purity was good from NMR analysis.

Separated HMF: 1H NMR spectrum (400 MHz, [D6] DMSO, δ ppm): 4.481-4.496 (d, 2 H, J = 6.000), 5.548–5.562 (t, 1 H, J = 5.600), 6.573–6.582 (d, 1 H, J = 3.600), 7.455–7.465 (d, 1 H, J = 4.000), 9.519 (s, 1H); 13C NMR spectrum (100 MHz, [D6] DMSO, δ ppm): 56.6,

110.3, 125.1, 152.4, 162.8, 178.6.

Characterization:

Field emission scanning electron microscopy (FE-SEM) was performed on a Hitachi S-4800 Scanning electron microscope at an accelerating voltage of 20 kV. The sample was prepared by drop-casting an ethanol suspension onto mica substrate and then coated with gold. Transmission electron microscope (TEM) was by a JEOL 1230 transmission electron microscope at an accelerating voltage of 75 kV. Samples dispersed at an appropriate concentration were cast onto a carbon-coated copper grid.

Energy dispersive X-ray spectroscopy (EDX) was taken on a JEM-2100F transmission electron microscope at an accelerating voltage of 200 kV. 1H NMR and 13C NMR spectra were obtained on a Mercury plus 400 MHz spectrometer with D6-DMSO as the solvent and tetramethylsilane (TMS) as the internal standard. Fourier transform infrared spectra (FT-IR) were recorded on a NEXUS-470 Fourier transform infrared spectrophotometer. Thermal gravimetric analysis (TGA) was run on a Pyris 1 TGA instrument. The TGA curves were measured under N2 by heating the samples from 50 to 800 °C at a rate of 20 °C min–1. All measurements were taken under a constant flow of nitrogen of 40 mL/min. Gas chromatography-mass spectrometry (GC-MS) were conducted with a Finnigan Voyager GC-MS equipped with a HP-5MS capillary column (30 m×0.25 mm×0.25 μm) and the corresponding GC/MS spectra. High performance liquid chromatography (HPLC) measurements are conducted using a Shimaszu Class-VP HPLC with RID-10A Refractive Index detector. A shodex SH1011 sugar column (300 × 8 mm, 6 μm) is used to separate the products. General HPLC conditions for analysis of HMF yield: column temperature: 50oC; rate of fluid: 0.8 ml / min; injection amount: 5 μL. The elemental analysis was taken on a vario EL Ⅲ analyzer (Elementar Company in Germany) in Shanghai Institute of Crganic Chemistry (SIOC), Chinese Academy of Sciences.

Experimental Data:

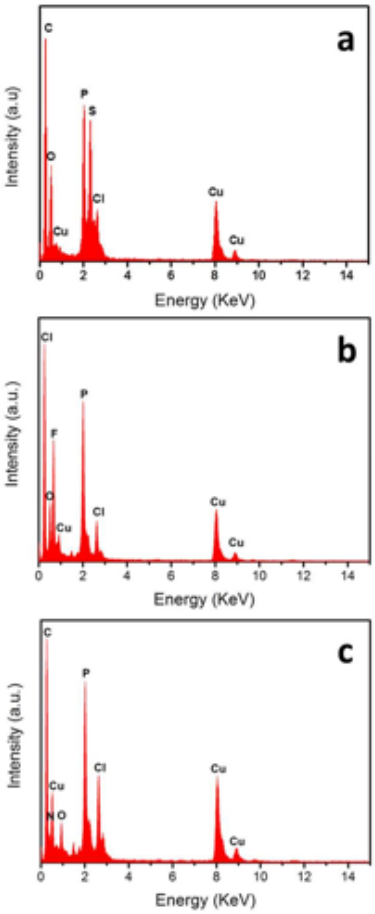

Element	Weight(%)	Atom(%)
C K	38.13	61.10
O K	10.24	12.32
P K	18.10	11.24
S K	13.95	8.37
Cl K	4.28	2.33
Cu K	15.29	4.63
Total	100.00	100.00

Element	Weight(%)	Atom(%)
C K	39.76	60.30
O K	6.08	6.93
F K	15.26	14.64
P K	19.45	11.44
Cl K	4.95	2.54
Cu K	14.50	4.16
Total	100.00	100.00

Element	Weight(%)	Atom(%)
C K	38.99	61.60
N K	5.73	7.76
O K	6.49	7.69
P K	19.13	11.72
Cl K	9.98	5.34
Cu K	19.69	5.88
Total	100.00	100.00

Fig. S1 Energy dispersive X-ray spectroscopy data of (a) PZS-3.5, (b) PZAF-3.5 and (c) PZODA-3.5.

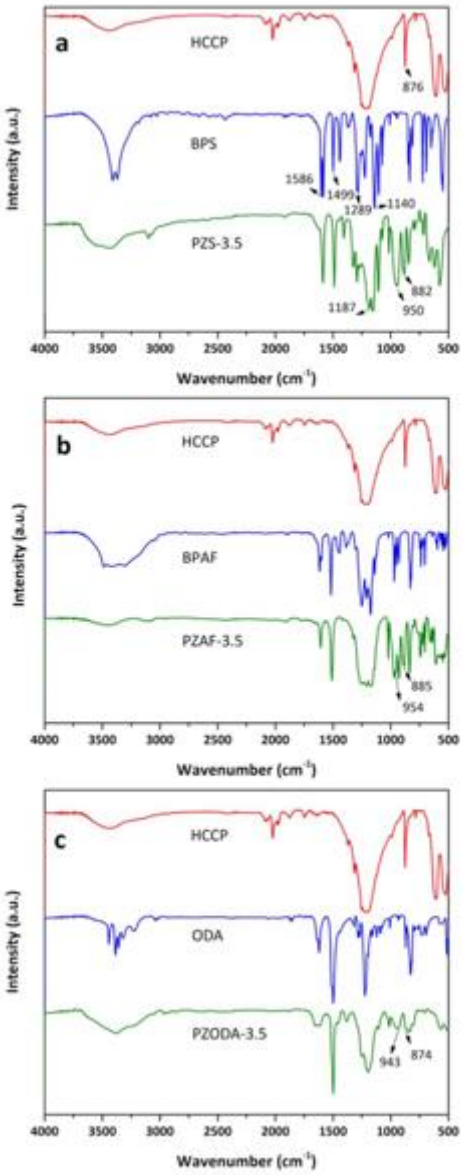

Figure S2. FTIR spectra of (a) PZS-3.5, (b) PZAF-3.5 and (c) PZODA-3.5 with the spectra of monomers.

The characteristic peak of HCCP monomer (P-N) is located at 876 cm-1. For BPS monomer, the characteristic peaks of (C=C(Ph)) are located at 1586 cm-1 and 1499 cm-1, while the characteristic peaks of (O=S=O) are located at 1289 cm-1 and 1140 cm-1, respectively. For PZS-3.5, the product show a new characteristic peaks of (P-O-(Ph)) are located at 945 cm-1, which verified the polymerization successfully. The retained the characteristic peaks of (P=N) at 1187 cm-1 and (P-N) at 882 cm-1, and other characteristic peaks of BPS monomer, verify the PZS-3.5 has the fundamental structure of HCCP and BPS units. The slight shift vibration frequency of (P-N) in HCCP from 876 cm-1 to 882 cm-1 should be ascribed to the inductive effect of substituted BPS co-monomer.

For the sample of PZAF-3.5, the characteristic peaks originated from HCCP and BPAF can be found in a range of 500 ~ 1700 cm-1, which indicates the basic components in PZAF framework. Furthermore, the vibration frequency of (P-N) in HCCP moiety shifts to 885 cm-1 and the vibration frequency of newly formed (P-O-(Ph)) in PZAF might be located at 954 cm-1. There might be a stronger inductive effect on the P-O bonding compared with that of PZS framework, which is caused by the –CF3 group containing co-monomer BPAF with a strong electron-withdrawing capability.

For the sample PZODA-3.5, the characteristic peaks originated from HCCP and BPAF can also be found in a range of 500 ~ 1700 cm-1, indicating the basic components in PZODA framework. And the vibration peak located at 943 cm-1 should be attributed to the bond formation (P-N-(Ph)) after the polymerization. However, the vibration peak at 874 cm-1, which can be regarded as the vibration of (P-N) in HCCP, slightly shifts to the lower frequency by comparing that of PZS and PZAF, and this might be due to the conjugated effect in ODA co- monomer with an electron-donating ability.

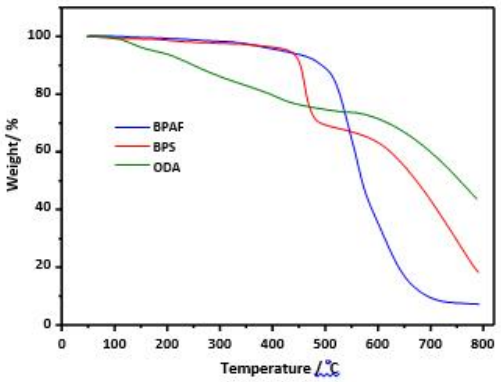

Fig. S3 The TGA profiles of co-monomers BPS, BPAF and ODA.

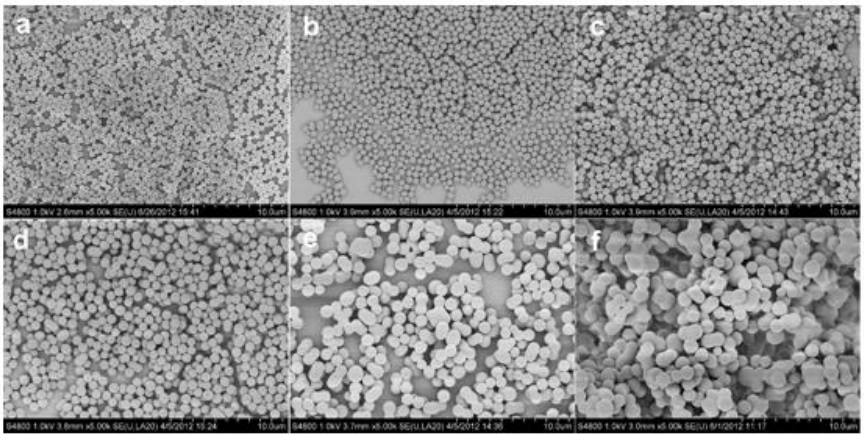

Fig. S4 FE-SEM images of PZS polyphosphazene nanoparticles with different BPS : HCCP molar ratio (a) 2/1, (b) 3/1, (c) 3.5/1, (d) 4.5/1, (e)5.5/1, (f) 7/1.

Table S1. Elemental Analysis (EA) results of PZS-NPs with different HCCP: BPS molar ratios.

sample	C /%	H /%	N /%	Cl /%
PZS-2.0	41.09	2.61	5.83	12.09
PZS-3.5	46.22	3.24	4.78	3.25
PZS-5.5	47.97	3.18	4.42	2.74
PZS-7.0	48.38	4.32	3.36	2.68

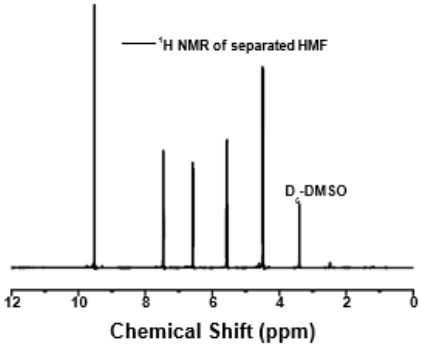

Fig. S7 ^{1}H NMR spectra of the separated HMF after reaction (PZS-2.0 1.25 g, fructose 1.25 g, DMSO 11.25 g, 90°C, 2h). ^{1}H NMR spectrum (400 MHz, [D_6] DMSO, δ ppm): 4.481-4.496 (d, 2 H, J = 6.000), 5.548−5.562 (t, 1 H, J = 5.600), 6.573−6.582 (d, 1 H, J = 3.600), 7.455−7.465 (d, 1 H, J = 4.000), 9.519 (s, 1H).

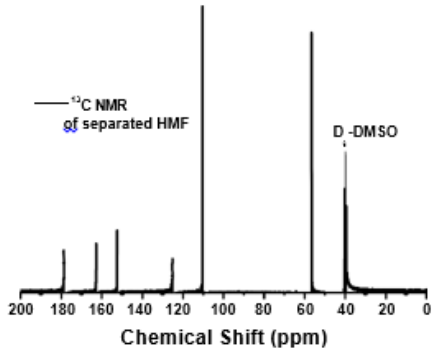

Fig. S8 ^{13}C NMR spectra of the separated HMF after reaction (PZS-2.0 1.25 g, fructose 1.25 g, DMSO 11.25 g, 90°C, 2h). ^{13}C NMR spectrum (100 MHz, [D_6] DMSO, δ ppm): 56.6, 110.3, 125.1, 152.4, 162.8, 178.6.

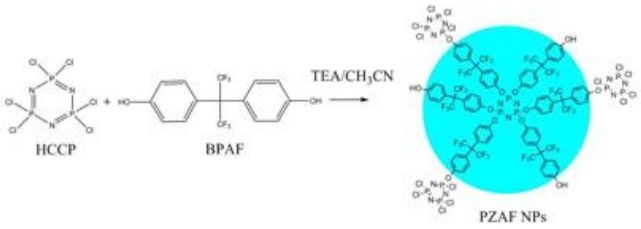

Scheme S1. The scheme illustrates the preparation of poly(cyclotriphosphazeneco-(4,4'- (hexafluoroisopropylidene) diphenol)) nanoparticles (PZAF-NPs).

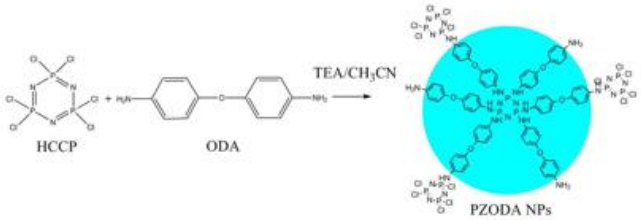

Scheme S2. The scheme illustrates the preparation of poly(cyclotriphosphazeneco- (4,4'-diaminodiphenyl ether)) nanoparticles (PZODA-NPs).

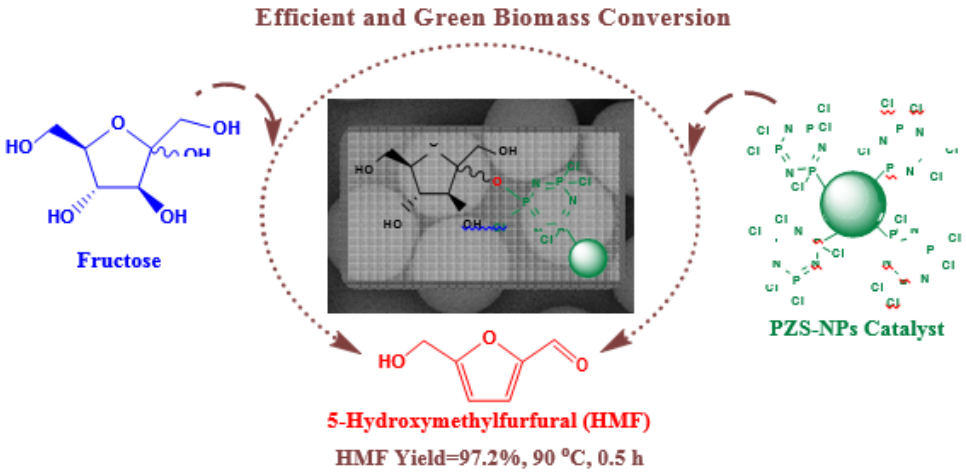

Magic polymer balls: Novel polyphosphazene nanoparticles (PZS-NPs) as a green heterogeneous catalyst are discovered for high yield conversion of fructose to hydroxymethylfurfural, which is due to the unique cyclotriphosphazene unit and the electron-withdrawing nature of the polymer backbone. This strategy will supply a new pathway for designing highly active heterogeneous catalysts as well as the innovative technologies for biomass conversion.

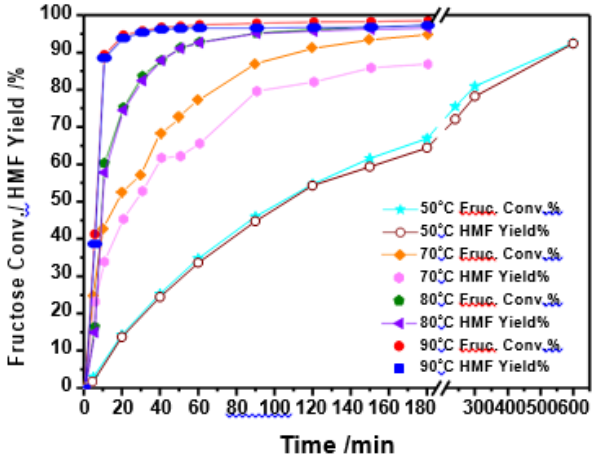

Fig. S5 The catalysis real-time data of PZS-3.5 with different reaction temperatures. Reaction conditions: 3 % D-fructose in DMSO, 0.2 g of catalyst, 3 – 10 h of reaction time.

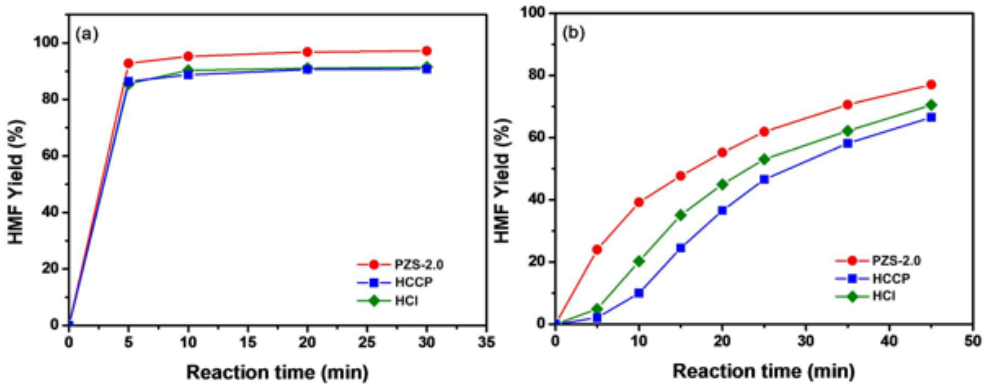

Fig. S6. Effect of reaction temperatures on conversion of fructose to HMF catalyzed by PZS-2.0, HCCP and HCl at (a) 90 °C and (b) 60 °C in 3 wt% fructose solution.